

**Supporting information to:**

**Chain length study of silver carboxylates in focused electron beam induced deposition**

Jakub Jurczyk, Katarzyna Madajska, Luisa Berger, Leo Brockhuis, Thomas E. J. Edwards, Katja Höflich, Czesław Kapusta, Iwona Szymanska, Ivo Utke

S1. Distribution of the impinging flux of precursor molecules as a fraction of the flux leaving nozzle exit

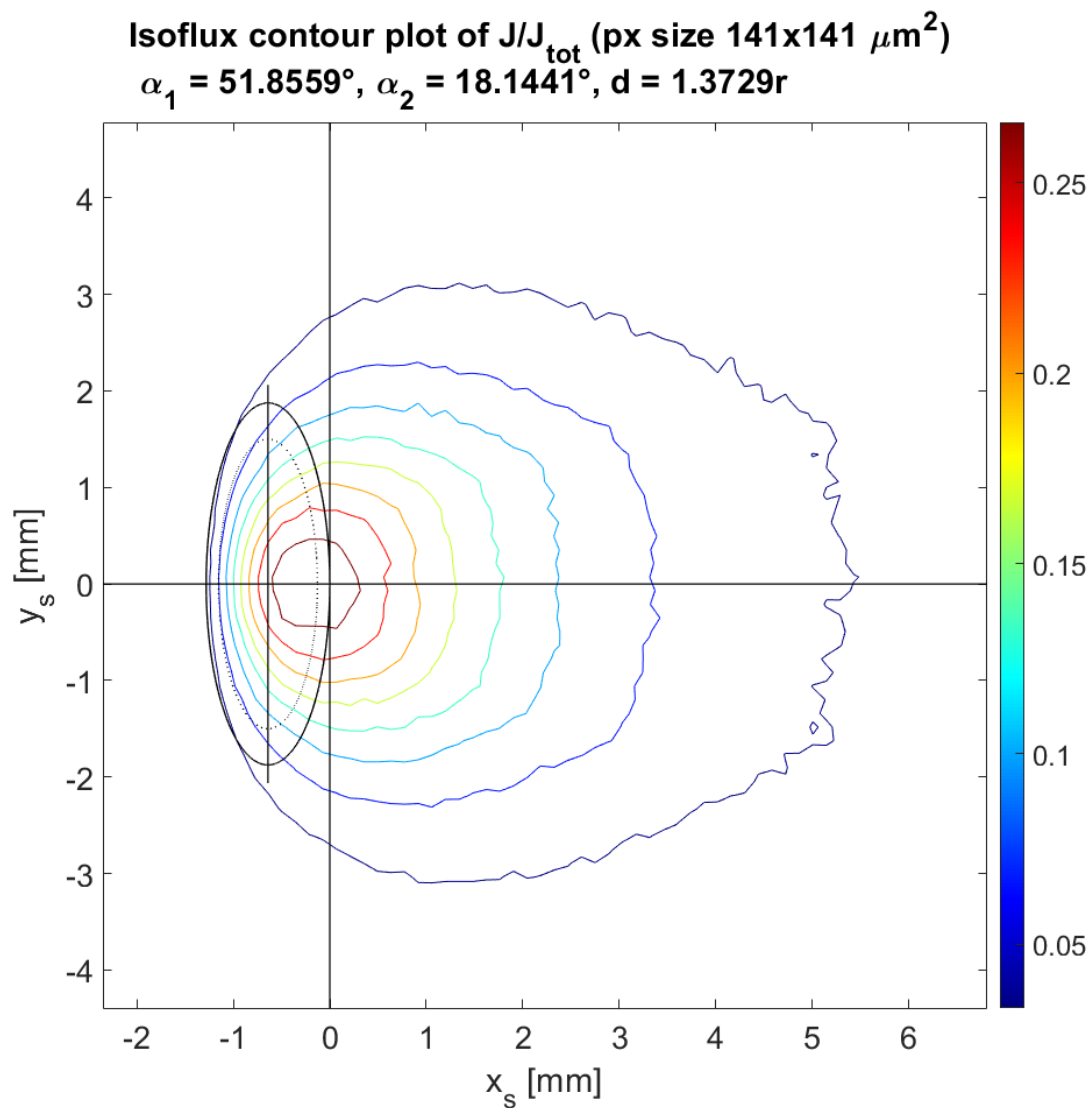


Figure S1 Distribution of the impinging flux of molecules as a fraction of the flux leaving nozzle exit.

All presented deposition experiments were performed around 0.2 mm of lateral distance from the upper edge of the nozzle exit, position here at 0 on the X axis.

S2. Comparison between measured SAED patterns and the ones of pure Ag and AgO  
[Ag<sub>2</sub>(μ-O<sub>2</sub>CCF<sub>3</sub>)<sub>2</sub>]

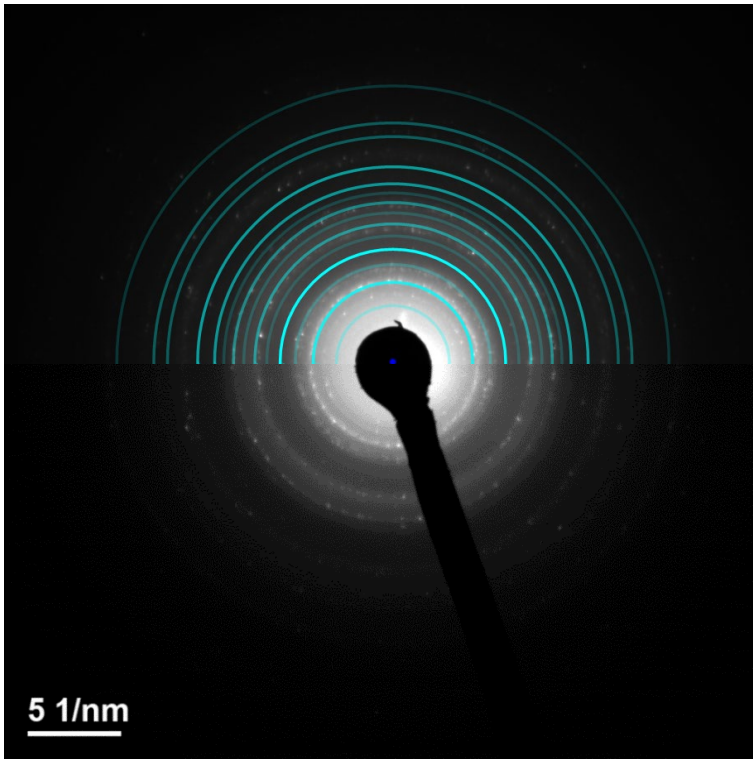


Figure S2.1 SAED pattern obtained from the deposit manufactured with [Ag<sub>2</sub>(μ-O<sub>2</sub>CCF<sub>3</sub>)<sub>2</sub>] compared to pattern of pure AgO (cyan rings).

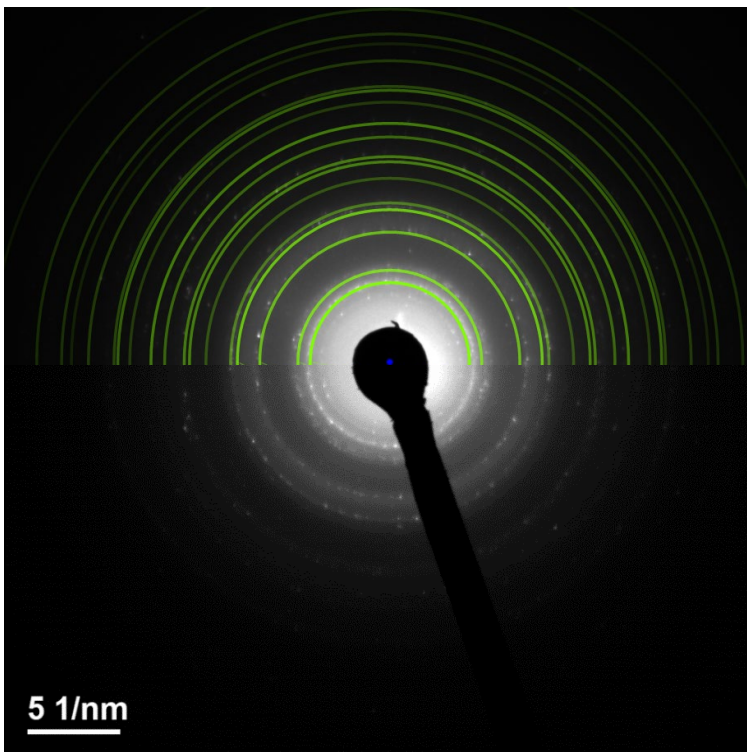


Figure S2.2 SAED pattern obtained from the deposit manufactured with [Ag<sub>2</sub>(μ-O<sub>2</sub>CCF<sub>3</sub>)<sub>2</sub>] compared to pattern of pure Ag (green rings).

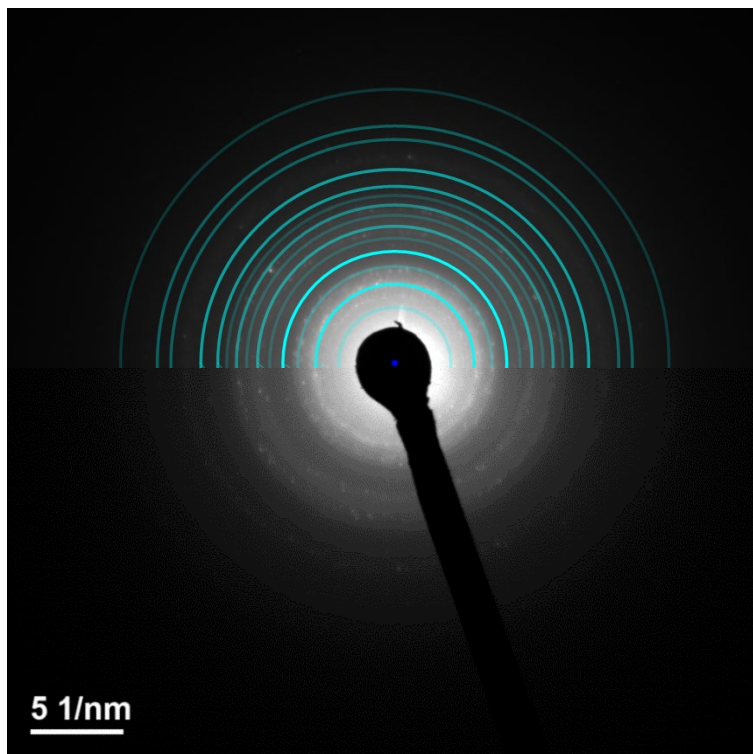
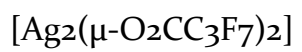


Figure S2.3 SAED pattern obtained from the deposit manufactured with  $[\text{Ag}_2(\mu\text{-O}_2\text{CC}_3\text{F}_7)_2]$  compared to pattern of pure AgO (cyan rings).

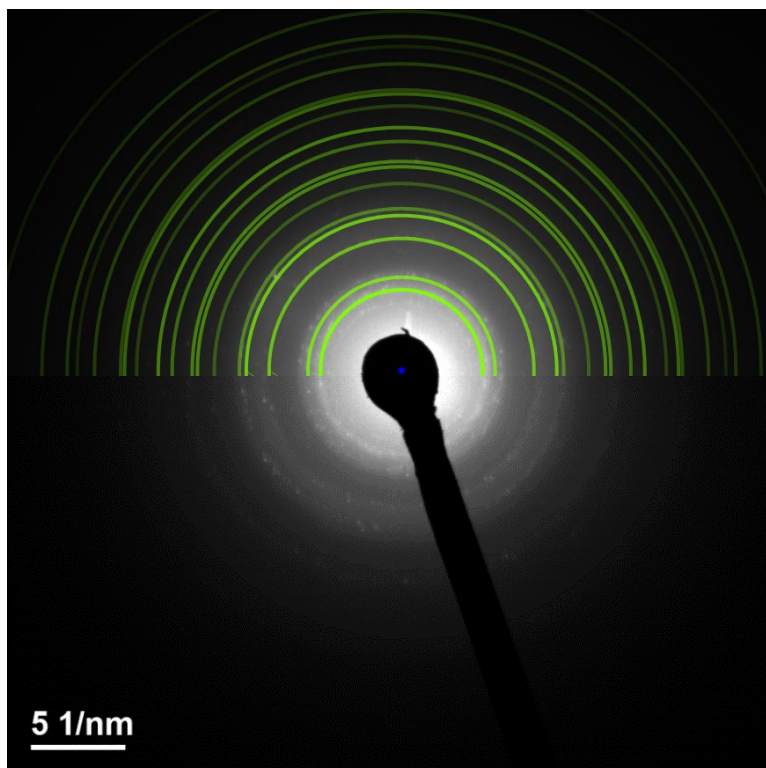


Figure S2.4 SAED pattern obtained from the deposit manufactured with  $[\text{Ag}_2(\mu\text{-O}_2\text{CC}_3\text{F}_7)_2]$  compared to pattern of pure Ag (green rings).

$[\text{Ag}_2(\mu\text{-O}_2\text{CtBu})_2]$

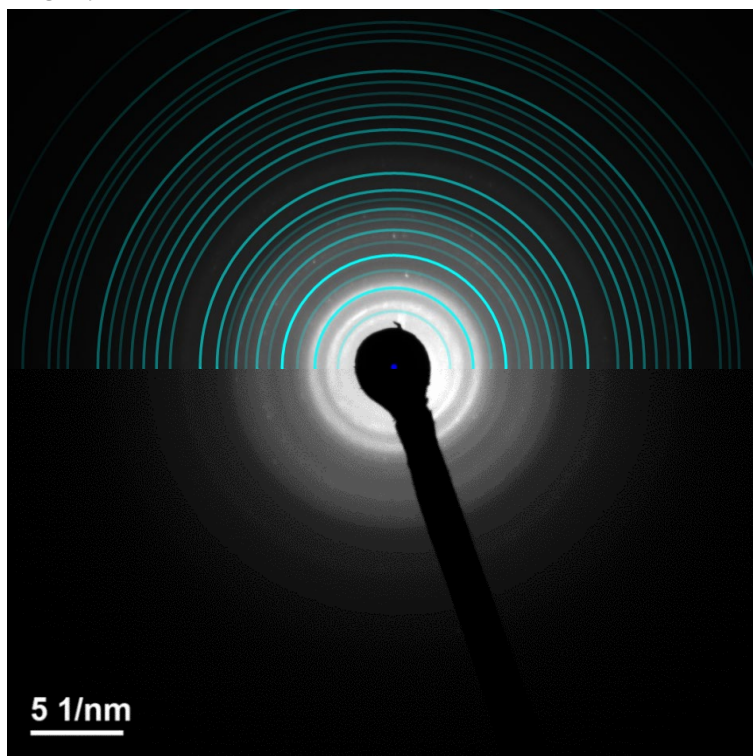


Figure S2.5 SAED pattern obtained from the deposit manufactured with  $[\text{Ag}_2(\mu\text{-O}_2\text{CtBu})_2]$  compared to pattern of pure AgO (cyan rings).

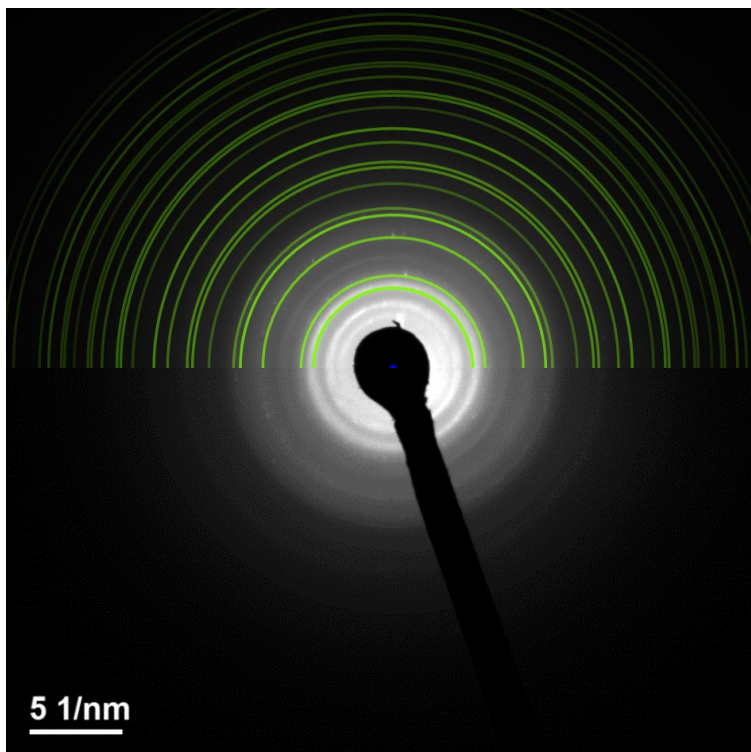


Figure S2.6 SAED pattern obtained from the deposit manufactured with  $[\text{Ag}_2(\mu\text{-O}_2\text{CtBu})_2]$  compared to pattern of pure Ag (cyan rings).

### S3. AFM of the spot deposits

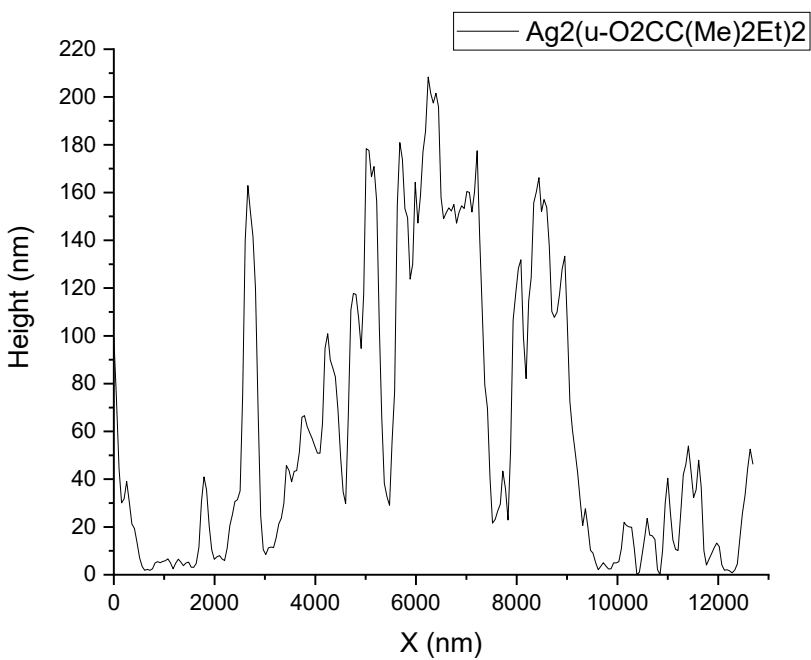


Figure S3.1 AFM profile of the spot deposit made with  $[\text{Ag}_2(\mu\text{-O}_2\text{CC}(\text{Me})_2\text{Et})_2]$ . Measured profile was lead through the center of the deposit.

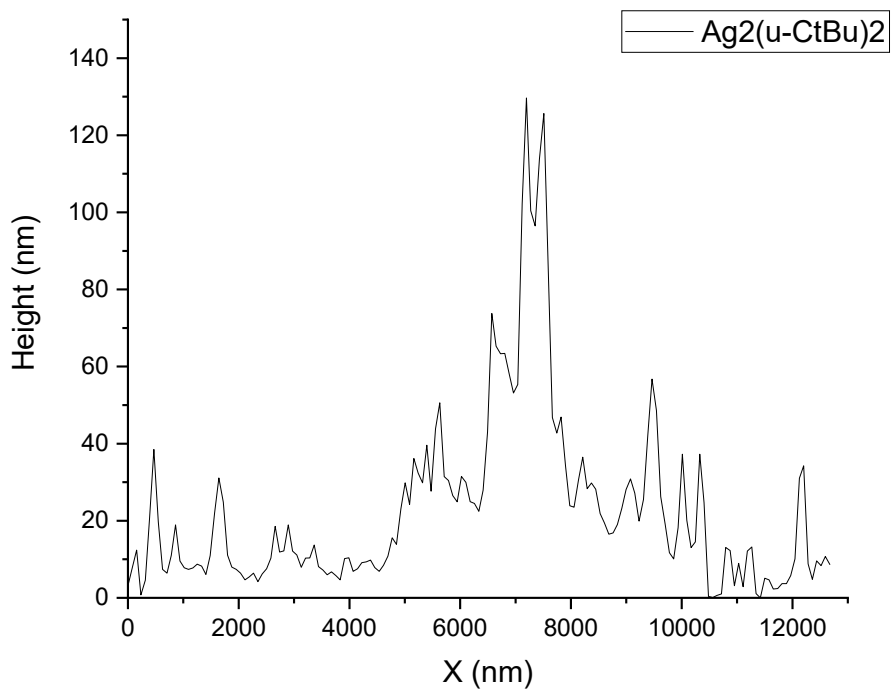


Figure S3.2 AFM profile of the spot deposit made with  $[\text{Ag}_2(\mu\text{-O}_2\text{CC}^t\text{Bu})_2]$ . Measured profile was lead through the center of the deposit.

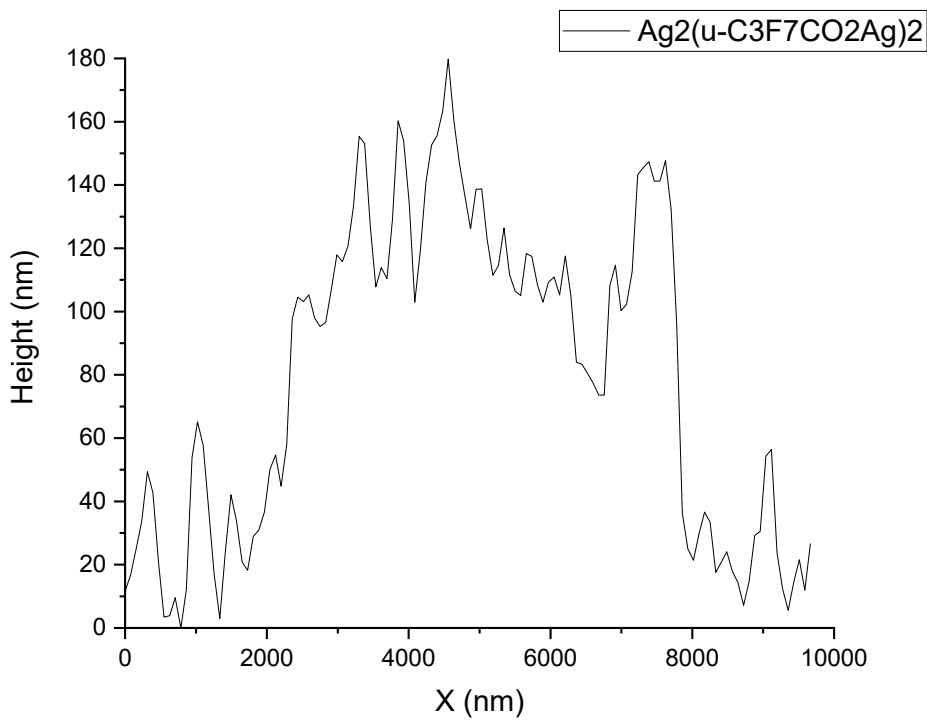


Figure S3.3 AFM profile of the spot deposit made with  $[\text{Ag}_2(\mu\text{-O}_2\text{CC}_3\text{F}_7)_2]$ . Measured profile was lead through the center of the deposit.

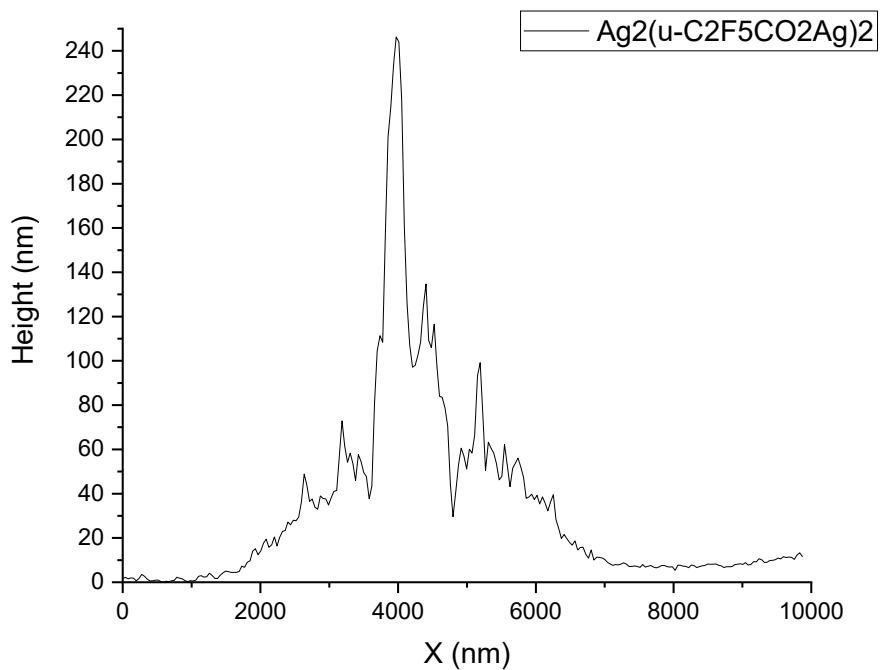


Figure S3.4 AFM profile of the spot deposit made with  $[\text{Ag}_2(\mu\text{-O}_2\text{CC}_2\text{F}_5)_2]$ . Measured profile was lead through the center of the deposit.

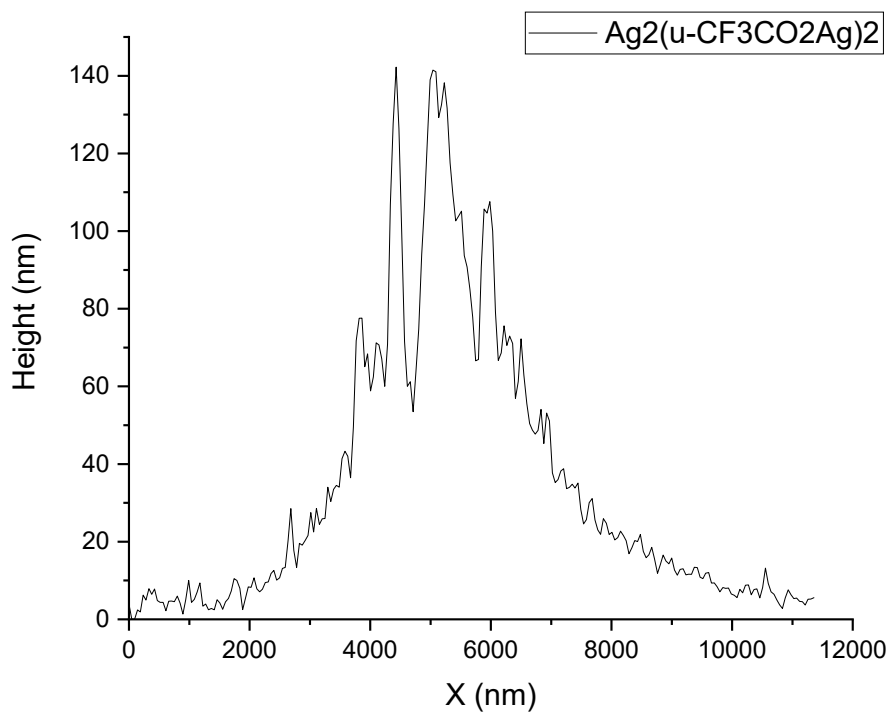


Figure S3.5 AFM profile of the spot deposit made with  $[\text{Ag}_2(\mu\text{-O}_2\text{CCF}_3)_2]$ . Measured profile was lead through the center of the deposit.

